



**HAL**  
open science

## **Influence of fine sediments on rheology properties of self-compacting concretes**

Nongwendé Philippe Ouédraogo, Frédéric Becquart, Mahfoud Benzerzour,  
Nor-Edine Abriak

► **To cite this version:**

Nongwendé Philippe Ouédraogo, Frédéric Becquart, Mahfoud Benzerzour, Nor-Edine Abriak. Influence of fine sediments on rheology properties of self-compacting concretes. Powder Technology, 2021, 392, pp.544-557. 10.1016/j.powtec.2021.07.035 . hal-04168098

**HAL Id: hal-04168098**

**<https://imt-nord-europe.hal.science/hal-04168098v1>**

Submitted on 22 Jul 2024

**HAL** is a multi-disciplinary open access archive for the deposit and dissemination of scientific research documents, whether they are published or not. The documents may come from teaching and research institutions in France or abroad, or from public or private research centers.

L'archive ouverte pluridisciplinaire **HAL**, est destinée au dépôt et à la diffusion de documents scientifiques de niveau recherche, publiés ou non, émanant des établissements d'enseignement et de recherche français ou étrangers, des laboratoires publics ou privés.



Distributed under a Creative Commons Attribution - NonCommercial 4.0 International License

# 1 **Influence of Fine Sediments on Rheology Properties of the Self-Compacting** 2 **Concrete**

3 Nongwendé Philippe OUEDRAOGO<sup>1, 2, 3, \*</sup>, Frédéric BECQUART<sup>1, 2</sup>, Mahfoud  
4 BENZERZOUR<sup>1, 2</sup>, Nor-Edine. ABRIAK<sup>1, 2</sup>

5 <sup>1</sup> Univ. Lille, ULR 4515 - LGCgE, Laboratoire de Génie Civil et géo-Environnement,  
6 F-59000 Lille, France

7 <sup>2</sup> IMT Lille Douai, F-59500 Douai, France

8 <sup>3</sup> Centrale Lille, UMR 9013–LaMcube–Laboratoire de Mécanique, Multiphysique, Multi-  
9 échelle, F-59000 Lille, France

10 \*Correspondence: [nongwende.philippe-ouedraogo@centrallille.fr](mailto:nongwende.philippe-ouedraogo@centrallille.fr)

11

## 12 **ABSTRACT**

13

14 Sediments from dredging works are increasingly used in the building and construction  
15 industry. One of the major difficulties of sediment valorization resides notably in the very  
16 heterogeneous composition of its fine particles. This paper focused on the rheological impacts  
17 caused by the use of uncontaminated raw marine sediment (RS) in Self-Compacting Concrete  
18 (SCC). The Densified Mixture Design Algorithm (DMDA) was used to optimize RS as a raw  
19 material in the granular structure of the SCC. The AFREM grout method was used to  
20 determine the saturation dose of the superplasticizer. The rheological tests were carried out to  
21 assess the influence of fine RS particles on the workability of SCC. The stability of SCC was  
22 found to be correlated with the high percentage of fine particles less than 125  $\mu\text{m}$  present in  
23 the RS. The fine nature of clays and the organic matter caused the increase in yield stress and  
24 plastic viscosity. The rheological tests were carried out to assess the influence of fine RS  
25 particles on the workability of SCC. The stability of SCC was found to be correlated with the  
26 high percentage of fine particles less than 125  $\mu\text{m}$  present in the RS.

27

### 28 **Keywords:**

29 Raw sediment

30 Organic Matter

31 Clay

32 Self-compacting concrete

33 Rheology

## 34 **1 Introduction**

35 In the 1980's in Japan, the research of specific rheological performance of concrete led to the  
36 appearance of self-consolidating concrete (SCC) [1] [2]. Very fluid, homogeneous, and stable  
37 the establishment of the SCC is very simplified for every type of application (vertical,  
38 horizontal, oblique) [3]. In France, **most of the SCC markets is** very weak: about 5% against  
39 2% on average in Europe. According to Aloia-Schawartzentruber [3], it **explains** due to the  
40 difficulties of their formulation and the cost of specific materials (mineral additions,  
41 superplasticizers, etc.). **Utilized** to insure the rheological properties. It will be more  
42 advantageous to formulate an SCC with reduced cost **utilizing** secondary raw materials.

43 In France, more than 50 million cubic meters of marine sediments are dredged every year [4].  
44 According to the regulation context, the management of this huge volume of sediments needs  
45 an adapted methodology and treatment processes before considering a **valorization** at large  
46 scale [5][6]. The Dunkirk port in France dredges each year about four million cubic meters.  
47 One of the strategic objectives is to find high add-value beneficial uses for large volume of  
48 dredged sediments [7]. **For more than a** decade, several experimental applications with  
49 sediments have been performed in public works, road construction, standard concrete and  
50 bricks, et. [8][9]. For cementitious materials, the classical approach is to partially replace the  
51 sand fraction or the cement fraction. Today, these applications do not yet incorporate  
52 **optimized** sediment rates somehow governed by the question of the environmental impact. In  
53 this context, considering the finesse of sediments, their **valorization** deserves to be studied as  
54 a commodity in SCC.

55 Harbour sediment is a material coming from the erosion of rocks, soils or/and chemical and  
56 biochemical precipitations. It is composed of natural and mineral elements (clay, silt, sand), of  
57 organic matter (plant debris, micro-organisms, humic colloids), as well as water. The particle  
58 size of sediment varies according to the dredging and the treatment process [10]. Silt, clay and  
59 a part of organic matter constitute the fine fraction of the sediment (< 63  $\mu\text{m}$ ). According to  
60 Gosselin [11], this fraction contains more of the contaminated pollutants (heavy metals,  
61 micropollutants, nutrients). The sand fraction of the sediment constitutes the largest part. Sand  
62 presents a grain size distribution and a porosity close to natural sand 0/2 mm. SCC  
63 formulation needs an important volume of paste (cement + superplasticizer + effective water  
64 + air), around 330 to 400  $\text{l/m}^3$  [12]. This volume of paste allows ensuring the fluidity,  
65 homogeneity and stability of the mixture. Nowadays, the most commonly used additions for  
66 the formulation of the SCC are calcareous or siliceous additions, metakaolins [2][13]. In

67 mass, their passing to 2 mm is equal to 100% and greater than 85% of the particles lower than  
68 125  $\mu\text{m}$  [12].

69 In the state-of-art, many studies have been carried out on the use of treated sediment in  
70 cementitious matrix [14]– [18]. For example, Amar et al. have shown that a physical grinding  
71 and the calcination of sediment before its use in a cementitious matrix allow to assimilate its  
72 behaviour to the one of additions (calcareous, siliceous) and to contribute to improving the  
73 mechanical properties of grouts [19], [20]. Rosière et al. [21] have shown that the use of  
74 sediment calcined at 650°C in the SCC allows improving the rheological and mechanical  
75 properties. To use the sediment in more large quantity of concrete, Agostini et al. [22] have  
76 been able to substitute 33% of the sand fraction with sediment in cementitious matrix with a  
77 treatment of the sediment according to the Novosol® process.

78 Thermal treatment of sediment presents some advantages [22]– [31] as:

- 79 • the elimination of some of the organic part,
- 80 • the improvement of the rheological properties of SCC,
- 81 • the removing sediment agglomerates during mixing,
- 82 • the obtaining short-term mechanical properties of non-bearing structures,
- 83 • the activating of pozzolanic properties in the long term,
- 84 • the **stabilization** of heavy metals.

85 In this study, for environmental and economic reasons (reduction of the cost of thermal and  
86 physical treatment), the **valorization** strategy was to experiment with the use of sediment in its  
87 raw state in the SCC formulation, without the classical mineral additions of this kind of  
88 concrete. Chemical analyses of the leaching test on the studied raw sediment concluded that  
89 this sediment is a non-inert non-hazardous waste according to the law 28 October 2010/CE.  
90 **This classification makes it possible legitimately to assume the hypothesis that a physical,**  
91 **chemical and thermal treatment is not necessarily mandatory for the use of sediment in**  
92 **cementitious matrices such as SCC in the present case.**

93 In this paper, the specific case of a SCC formulation incorporating about 300  $\text{kg}/\text{m}^3$  of RS  
94 with an initial water content of 15 to 20% was tested. The SCC properties in the fresh state  
95 give us spreading of SF1 class (550 to 650 mm) and SF2 (660 to 750 mm) according to the  
96 classification of the AFGC guideline [12].

97 It is well known that best rheological properties of SCC are achieved when **optimizing**  
98 parameters such as the compaction index of the mixture, the superplasticizer dosage, the

99 shape and fineness of the components. The rheological properties of fresh concrete according  
100 to Ovarlez and Rossel are often **characterized** by the Bingham model (Eq.1):

$$\tau = \tau_0 + \eta \cdot \dot{\gamma} \quad (1)$$

101 Several geometries make it possible to evaluate the yield stress of a simple (simple shear  
102 flow) or complex suspension. The most standard geometries used are parallel plates, cones,  
103 and plates, quilts. The parallel geometry is used for the measurement of SCC slurry flow. This  
104 geometry is suitable for suspensions whose largest elements are less than 200 microns. Its  
105 application has advantages such as the use of a small quantity of the paste for the  
106 measurements, the free fixing of the height of the gap, and permits to maintain the suspension  
107 homogeneity during the measurement of the yield stress while avoiding considering the  
108 effects of friction between the suspension and the sidewalls of the geometry [32].

109 The purpose of this article is to show the experimental feasibility of a SCC with sediment  
110 (**optimized** quantity) and without standard mineral additions. **A specific paste rheometer was**  
111 **used to evaluate the impact of the sediment fines fraction on the rheological behavior of the**  
112 **different SCC pastes.** Comparisons of yield stress, viscosities, and SEB observations have  
113 been **realized** to quantify the influence of sediment on the SCC mechanical and rheological  
114 properties.

## 115 **2 Materials and protocols**

### 116 **2.1 Materials**

#### 117 **- Sediment characterization**

118 **The raw sediment in its granular composition is not considered a mineral addition. A granular**  
119 **separation of the raw sediment in two fractions (Fig.1.), respectively the passing to 125µm**  
120 **sieve (noted F1) and the refusals to 125 µm sieve (noted F2), shows a difference in properties**  
121 **(physical, geotechnical and mineralogical). The properties of the F1 fraction are closer to the**  
122 **additions used in standard concrete, as shown in Figure 2 concerning the grain size**  
123 **distribution. By experimental feedback about the properties of Dunkirk Port sediments, the F1**  
124 **fraction approximately stands for 25 to 60% of the raw sediment. This F1 fraction without any**  
125 **treatment can play the role of a mineral pseudo-addition.**

126 The sediments have been dredged from the Grand Port Maritime of Dunkerque (GPMD)  
127 located in the North of France. RS is used in the initial water content of 15 to 20% in SCC  
128 without any physical or thermal treatment. Leaching tests in electrochemistry allow the pH

129 evaluation of 8 to 20 ° C. True density was 2.65 g / cm<sup>3</sup> measured by helium pycnometer,  
130 which is approximately equal to that of 0/4 natural sand. The methylene blue and size  
131 distribution test shows that the RS contains 34.30% clay-silt mixture and 61.47% sand. The  
132 organic matter (OM) was measured as 3.33% using the standard XP P94-047 by calcination in  
133 an oven at 450 ° C for 3 hours. This conformed to the result of 2.1% of total organic carbon  
134 (OC) measured using the standard NF EN 13137 which according to Pribyl et al. OC / OM  
135 must be between 1.4 and 2.5 [33].

136 The chemical composition of the sediment determined by X-ray fluorescence Table 2 shows  
137 that the main chemical elements in the sediment were oxygen containing 52.1%, silicon  
138 28.2%, calcium 10.5% and aluminum 2.9%. The value of PAHs (polycyclic aromatic  
139 hydrocarbons) was 6.620 mg / kg and that of PCBs (polychlorinated biphenyls) was 0.55 mg /  
140 kg, which was lower than the limited value according to Table 3 of the national decree of 12  
141 December 2014.

142 RS was used as a secondary raw material in the SCC. Grout particles smaller than 2 mm  
143 participated in the mixing. The reconstitution of the granular elements of the SCC paste, the  
144 particle size distribution by wet sieving in accordance with XP P 94-041, allowed for a sieve  
145 size of 125 µm (fraction F1). Fig. 2. shows the particle size curve of F1, which is close to  
146 CEM III / A 42.5. According to the AFGC, the F1 fraction contributes to the volume of the  
147 paste and influences the rheological and mechanical properties of the SCC [12]. The technical  
148 size distributed by wet sieving allows maintaining the organic matter in the SCC paste and  
149 also avoid sediment agglomerates that appear during the drying process. It has made it  
150 possible to preserve the shape of the grains of the F1 fraction during rheological  
151 measurements.

#### 152 - **Other Materials**

153 Slag-blended cement CEM III / A 42.5 N was used to produce SSC in this study. It is  
154 composed of 54% clinker and 43% slag-blended. This cement has an alkali content lower than  
155 Portland cement and allows the stabilization of traces of heavy metals in the cement matrix.  
156 The chemical compositions of this material are given in Table 2. Crushed coarse aggregate  
157 ( $D_{max}$  11.2 mm, density 2.45, water absorption capacity 0.43% and unit weight 1389 kg / m<sup>3</sup>)  
158 and natural sand (modulus of fineness 2.71, density 2.64, absorption capacity 1.1% and unit  
159 weight 1645.8 kg / m<sup>3</sup>) were used. Superplasticizer was a high-efficiency polycarboxylate-  
160 based with the density of 1.05 g / cm<sup>3</sup>. **This type of high-performance water reducing**

161 **admixture** (HRWRA) has been used to reduce viscosity and improve workability in different  
162 mixtures [34].

## 163 **2.2 Mixtures' proportioning**

164 The densified mixture design algorithm (DMDA) was applied for concrete mix design to  
165 study the feasibility of using marine sediments in SCC [35][36]. DMDA incorporating  
166 mineral addition is used to fill the void of aggregates and hence increase the density of the  
167 aggregate system. RS used does not partially replace cement or sand but acts physically as  
168 filler and creates a nucleation effect for C3A hydrates in the cement paste [37]. The maximum  
169 weight ratio  $\alpha_{max}$  of blended sand and sediment can be expressed as:

$$\alpha_{max} = \frac{W_{se}}{W_{se} + W_{sa}} \quad (3)$$

170 Where  $W_{se}$  is the density of sediment in  $\text{kg/m}^3$  and  $W_{sa}$  is the density of sand in  $\text{kg/m}^3$ .

171 The weight ratio  $\beta_{max}$  at the maximum loose, dry density can be expressed as:

$$\beta_{max} = \frac{W_{sed} + W_{sa}}{(W_{sed} + W_{sa}) + W_{ca}} \quad (4)$$

172 Where  $W_{ca}$  is the density of coarse aggregate,  $\text{kg/m}^3$ .

173 The minimum cement paste volume ( $V_p$ ) can be estimated as:

$$V_p = V_v + S * t = nV_v = n(1 - \sum \frac{W_i}{\gamma_i}) \quad (5)$$

174 Where  $S$  is the surface area of aggregates,  $\text{m}^2$ ;  $t$  is the thickness of lubricating paste on the  
175 surface of aggregate,  $\mu\text{m}$ ;  $V_v$  is the smallest void among aggregates,  $\text{m}^3$ ;  $W_i$  is the weight of  
176 aggregate,  $\text{kg/m}^3$ ; and  $\gamma_i$  is the density of aggregate,  $\text{kg/m}^3$ .

177 The water-to-binder ratio (W/B) is calculated as following:

$$\lambda = \frac{W_w}{W_B} = \frac{W_w}{W_c + W_{sed}} \quad (6)$$

178 Two coefficients  $n$  were used in the DMDA algorithm to obtain the required workability. The  
179 values of  $n$  ( $n = \frac{V_p}{V_v}$ ) were 1.164 and 1.189. These values correspond to a W/B ratio of 0.48  
180 and 0.46. Fig. 4.

181 The grouts were formulated by the AFREM method Fig. 3. [38] They were deduced from that  
182 of the concrete by removing all elements larger than 2 mm, together with the water they

183 absorb. The relationship between SCC and grout by the AFREM grout by the AFREM  
184 method is in the hypothesis that the two complex suspensions are linked by their viscosities  
185 according to Farris's mode:

$$\eta_{concrete} = \eta_{paste} * f(V_p, CA/FA) \quad (7)$$

186

187 Where  $V_p$  is the volume of binding paste and CA/FA the coarse/fine aggregate ratio.

188 The pastes were deduced from that of the grout by removing all elements larger than 125  $\mu\text{m}$ ,  
189 together with the water they absorb. By making the assumption that the saturation proportion  
190 is the same, we can write:

$$\eta_{grout} = \eta_{paste} * f(V_p, CA/FA) \quad (8)$$

191

192 **The viscosity of the paste is the one that influences the rheological behavior of the grout.** Fig.  
193 3. and Fig. 4. **illustrates the method of describer used to move from SCC to paste.**

### 194 **2.3 Experiments on Grouts**

195 For each W/B, the proportions of the F1G and F2G grouts are presented in the **Table 4**. The  
196 RS was used in a first state, dried in an oven at 105 ° C to arrive at a constant mass, and a  
197 second state where the initial water content of 15% to 20%.

198 Procedure of saturation of grouts is as follows Fig. 6.

- 199 ✓ The first step of mixing consists of preparing the raw sediment to eliminate as much as  
200 possible the agglomerates:
- 201 - Introduce into the bowl the sediment and a quantity of water necessary to reach the  
202 standard consistency. **The standard consistency is measured using the Vicat apparatus**  
203 **equipped with a 10 mm diameter consistency probe as defined in standard NF EN 196**  
204 **- 3 + A1. This consistency corresponds to the water content of the paste which allows**  
205 **obtaining a penetration of the probe of 30 mm  $\pm$  2 mm, that is to say a reading of 10**  
206 **mm  $\pm$  2 mm.** The water demand for the RS evaluated according to the standard NF P  
207 18 – 508 is 28.5%.
  - 208 - Mix at high speed for the 60s.
  - 209 - Mix in slow speed for 15s while introducing passers to 2 mm of natural sand 0/4.
  - 210 - Mix for 45s at high speed. During this period, the sand grains will shear the maximum  
211 agglomerates of RS, this is a point that will be discussed below.



212 The 5 liters stainless steel mixer had an electronic variable speed drive. The slowest speed  
213 was 62 rpm and the highest speed was 125 rpm.

214 ✓ The second stage of mixing includes the introduction of other constituents while  
215 conserving flow time measurements and also following the protocol established by the  
216 AFREM method.

#### 217 **2.4 Experiments on SCC**

218 The proportions of the different SCCs are shown in the Table 4. The RS is used in an initial  
219 water content of 15% to 20%. The choice of abandoning dried sediment for the formulation of  
220 concrete results from the last saturation dosages of the superplasticizer, the explanations are  
221 given below.

222 The total mixing time of SCC is 5 min. The Sediment preparation is always necessary to  
223 remove agglomerates. We use a 60-liter IGM concrete mixer at a constant speed, the mixing  
224 protocol is as follows:

- 225 • Introduce the RS and the amount of water required to reach the standard consistence  
226 (this water is removed from the total mixing water). Mix for 60s.
- 227 • Introduce the natural sand 0/4, mix for the 30s
- 228 • Introduce the gravel and mix for the 30s.
- 229 • Introduce 2/3 of the rest of the water, keep mixing for the 60s.
- 230 • Put the cement and diluted superplasticizer into 1/3 of the remaining water. Mix for  
231 the 4 min.

232 After mixing, the workability of fresh concrete is measured by the slump test using the  
233 Abrams cone according to EN 12350-2. For each mix F1C and F2C, nine cylindrical  
234 specimens (Ø110mm x H220 mm) (NF EN 12390-1) were cast to determine the compressive  
235 strength (NF EN 12390-3 standard). All SCC were cast without vibration and were treated in  
236 the laboratory at  $20 \pm 2$  ° C for 24 h. There was no delay in setting time. After that, all the  
237 cylinders were made in 90 days.

#### 238 **2.5 Experiments on Paste**

239 Sand with a grain size of less than 125 µm are dried in an oven at 105 ° C to a constant mass.  
240 2 kg of RS is sieved at 125 µm by size distribution by wet sieving and maintained at a water  
241 content of 17%. Sand fines are obtained by size distribution at 125 µm according to NF EN

242 12948. All materials were covered in the laboratory at  $20 \pm 2$  ° C for 24 h before the  
243 rheological tests.

244 - For SCC paste, sand and cement are mixed for 30 seconds. Then RS is introduced and  
245 the mixture mixed for 30s. Finally, we introduce the water and the superplasticizer and  
246 then the whole paste is homogenized by hand for 60 s. The total mixing time is 2 min.  
247 The mixture is left standing and the first measurements are taken 5 minutes after  
248 mixing (Fig. 5).

249 - For the other pastes indicated in the Table 6, they are turned for 2 min and allowed to  
250 stand for 5 minutes before the measured ones.

251 After mixing, a small amount of paste is used for each shear stress and viscosity  
252 measurement. The sample for the measurements is said to be homogeneous if the thickness of  
253 the paste is 5 times greater than the largest diameter of the grains  $D_{max}$ .

254 The slump of mortar was measured with Abrams' mini-cone. The yield stress as well as the  
255 plastic viscosities are measured for a ratio  $W / X = 0.46$  and  $0.48$  ( $X = C, F, S_{ed}, C + S_{ed}, C +$   
256  $F$ ). The names of the different pastes are shown in the Table 6.

## 257 **2.6 Measurements procedures**

### 258 **2.6.1 Rheological measurements**

259 The rheometer used is Anton Paar Modular Compact Rheometer MCR 102 equipped with a  
260 parallel plate geometry, the sample is put between two disks of the same symmetry axis and  
261 of same radius  $R = 12.5$  mm, separated by a gap  $H = 1.25$  mm. the shear rate  $\dot{\gamma}(r)$  (**Eq.9**)  
262 depends only on the radius  $r$ . The velocity of a radius  $r$  is  $\Omega r$  on the upper plate and zero on  
263 the lower plate, leading to Fig. 5.

$$\dot{\gamma}(r) = \frac{\Omega r}{H} \quad (9)$$

264 We can compute exactly shear stress  $\tau(r)$  as:

$$\tau(r) = 2 \frac{T}{\pi R^3} \frac{r}{R} \quad (10)$$

265 The measurement procedure is similar to the one used in L. Ducloué et al. [39]. The linear  
266 regression according to the Bingham model (Eq. 1) is done, the sample was then submitted to  
267 an increasing shear strain ramp from  $0 \text{ s}^{-1}$  to  $0.1 \text{ s}^{-1}$  during 30 s. The rheometer records the  
268 enhanced yield stress and plastic viscosity, as well as the structural build-up of the static yield

269 stress. When the structure broke down, the rheometer was stopped letting the paste rest for 15  
270 min until the next stress growth (Fig. 5). This was continued until a total of 60 min.

271 Pre-shearing was carried out 5 minutes before the first yield stress measurement. The pre-  
272 shearing allowed for a homogeneous placement of the material in the parallel plates as well as  
273 a deflocculation of the fine particles.

### 274 2.6.2 SEM observation

275 SEM observations were made on fragments. The RS fragments are obtained by drying in an  
276 oven at 105 ° C and passed to the 125 µm sieve. The SCC paste fragments are curing for 7  
277 days and then oven-dried at 40 ° C. The dimensions of the fragments are about 0.5 \* 0.5 cm.  
278 They are polished and metallized with carbon to observe their microscopic structures. SEM  
279 images in Back-Scatter Detector (BSE) mode are shown in Figure 16 and Figure 17.

## 280 3 Results and discussion

### 281 3.1 Fresh properties of grouts

282 The saturation curves of the grouts are presented in Fig. 7. An analysis of the demand for  
283 superplasticizer ( $Sp^*$ ) as a percentage of dry extract of the cement weight allow us to deduce  
284 that:

$$(Sp^*)_{F1G} = 0.90 > (Sp^*)_{F2G} = 0.65 \quad (11)$$

285 From our table formulations, F1G and F2G it shows that:

$$(W/B)_{F1G} = 0.48 > (W/B)_{F2G} = 0.46 \quad (12)$$

286

$$(V_{sed} + V_c)_{F1G} = (V_{sed} + V_c)_{F2G} = 300 \text{ l/m}^3 \quad (13)$$

287

$$(V_s)_{F1G} > (V_s)_{F2G} \quad (14)$$

288

289 Where  $V_s$  the volume of sand is,  $V_{sed}$  is the volume of sediment and  $V_c$  is the volume of  
290 cement.

291 From (Eq. 11)(Eq. 12)(Eq. 13)(Eq. 14), F1G should require less superplasticizer because it  
292 contains more water and more fine sand. To better understand, we calculated the saturation  
293 dose of RS ( $Sp^*_A$ ). The saturation dose of cement CEM III / A 42.5 in alone ( $Sp^*_C$ ) is 0.38%  
294 in dry extract of the weight of the cement which makes it possible to deduce:

$$Sp^*_A = (100 \times Sp^*_{c+A} - (100 - A\%) \times Sp^*_c) / A\% \quad (15)$$

295 Where A% is the percentage of sediment in each **Table 5** of the grout. It is deduced that  $Sp^*_A$   
 296 is 2.55% and 1.55% respectively for F1G and F2G. The results of saturation doses of the  
 297 grouts are confirmed. The mass percentage of sediment in F1G is higher than that of F2G,  
 298 which justifies the higher need for superplasticizer.

299 The paste volume of each grout is greater than 15%, the optimization of 80% saturation  
 300 dosage ( $Sp^*$ ) is indicated. It says that:

$$\frac{Sp}{Sp^*} = 0.80 \quad (16)$$

301 The values of Sp are indicated in the Table 4 and used to characterize the rheological  
 302 properties. The slump value of F1G and F2G shrinks little by little over time. An addition of  
 303 RS brings about a slower increase in structural viscosity of grout in time Fig. 7. Despite the  
 304 elongated mixing time to remove agglomerates, we observe the presence of agglomerates for  
 305 formulations whose RS has been dried at 105 ° C. The slump value of these nuts diminishes  
 306 because of the agglomerates.

### 307 **3.2 Properties of SCC**

308 The fresh density of concrete was 2378, 2371kg/m<sup>3</sup> for F1C, F2C respectively. **The**  
 309 **workability of the concrete was assessed by measurements of slump flow. The flow of SCC in**  
 310 **an unconfined area is characterized by the Abrams cone flow. They were** 690, 680 mm for  
 311 F1C and F2C respectively Fig. 9. [12]. There was no segregation or bleeding. We can deduce  
 312 that an increase in the amount of sediment implies an increase in the dosage of the water and  
 313 the superplasticizer. The fine particles of RS were limited to the bleeding phenomenon.  
 314 Fig.10. present the compressive strengths of SCC (average values obtained by three  
 315 measurements for compressive strength). Compressive strengths of F1C and F2C after 90  
 316 days increased. At 28 days they were 21, 25 MPa for F1C, F2C respectively. At 90 days, there  
 317 was an increase in resistance of 10 to 15%. F1C and F2C respect the specifications for the  
 318 construction of nonstructural works.

### 319 **3.3 Fresh properties of paste**

#### 320 **3.3.1 Yield stress variation and Viscosity Measurements**

321 The structural build-up for RS paste, cement paste, filler paste for paste symbols WS<sub>ed</sub>, WC,  
 322 WF respectively was illustrated in Fig. 11. The yield stress of WS<sub>ed</sub> is higher than that of WC

323 and also the paste WF. The WCS<sub>ed</sub> and WCF paste allows us to analyze the rheological  
324 behavior of the cement / RS complex Fig. 12.

325 It follows that the volume replacement at a rate t = 28% of a portion of the cement WC paste  
326 by sediment causes an increase in the yield stress figure. These results also explain the need  
327 for water and high superplasticiser for F1C grout and SSC F1C. However the opposite  
328 phenomenon is observed for the filler. Because when the volume is replaced at the same rate a  
329 portion of the cement of the paste WC. In the filler, there is a decrease in the yield stress (Fig.  
330 11). L. Rudzinski in his thesis explains that the introduction of mineral additions brings a  
331 reduction in fluidity. By substituting the volume of a portion of the cement/sediment complex  
332 with sand fines, without increasing the amount of water, the WCS<sub>ed</sub>S paste is obtained. It is  
333 found that the presence of fine sand allows the reduction of the yield stress (Fig. 13). The  
334 resulting F1P and F2P paste of SCC F1C and F2C respectively, have lower yield stress  
335 compared to the rest. The introduction of the superplasticizer decreases the yield stress and  
336 facilitates the slumping of the pastes (Fig. 12)

337 Plastic viscosities presented in the figure are measured after 45 min of formulation. Fig. 14.  
338 shows that the presence of the sediment makes the paste more viscous. One can observe a  
339 non-linear, approximating exponential increase in F1P and F2P viscosity. The provision of a  
340 viscosity agent was not required for sediment-based formulated concrete.

### 341 3.3.2 Slump Measurements

342 After 45 minutes of mixing, the mini-slump flow value of the F1P and F2P paste were 91.63  
343 and 79.17 cm respectively. The theoretical slumps are calculated using yield stress data  
344 collected by the rheometer. According to Coussot and Roussel, the yield stress is linked to  
345 slump by the following formula [40]:

$$\tau_0 = \frac{225\rho g\Omega^2}{128\pi^2 R^5} \quad (17)$$

346 The theory slump value of the F1P and F2P paste were 86.77 and 80.98 respectively. Fig.15.  
347 shows the parts of the different slump. The comparison of the experimental results with the  
348 theoretical results supports the validity of the theological program of the study.

349 Furthermore, the maintenance of workability is explained by the presence of the clay fraction  
350 in the SR. The illites present in the sediment can bind the calcium ions released by the cement  
351 and thus help to reduce hydrate formation. The modification of the hydration kinetics of the  
352 cement causes a delay in the setting time of the cement and a maintenance of the viscosity.

353 **3.4 Microstructural properties of Paste**

354 The OM content of 3.33% comes mainly from the calcination in the oven at 450 ° C from  
355 plant debris. The BSE SEM (Fig.16. and Fig.17.) of the RS shows the presence of  
356 microparticles of elongated shapes. This is the vegetable organic matter as discussed by K. H.  
357 Moa et al. , the rheology of cement-based materials is dependent on many parameters  
358 including the presence of fibers [41]. The presence of fiber oriented in all directions increases  
359 the shear strength [41].

360 In the same way, the organic matter consists mainly of humus, divided into fulvic acids and  
361 humic acids. This phase of organic matter represents 80 to 90% of the total organic carbon  
362 (TOC) of RS. The presence of these acids disturbs the hydration of the cement and leads to a  
363 modification of the rheological behavior of SCC in the fresh state.

364 In addition, we observe shell remains in the RS, their porous structures and irregular shapes  
365 influence the water demand in the RS (Fig. 16) These elements are present in the F1P and F2P  
366 pastes. After hydration of the cement, it is observed that a thin layer of cement paste covers  
367 some irregular shapes of the shell (Fig. 17) This probably explains the decrease of the yield  
368 stress during the introduction of the cement in the WS paste [42].

369 **4 Research significance and recommendation for the use of fine sediments in SCC**

370 The problem of sediment incorporation in self-compacting cementitious materials lies mainly  
371 in their very heterogeneous characteristics, particularly the presence of organic matter, clays  
372 and shells. The classical approach to the use of sediments in self-compacting concrete consists  
373 of partially replacing cement fraction with calcined and crushed sediments. The present study  
374 proposes an innovative approach that consists of partially substituting part of the sand with  
375 raw sediment from active lagoons. Through the results of this study, several recommendations  
376 can be made. It is suggested to:

- 377 - Conduct an environmental assessment of the RS before use. Indeed, the presence of  
378 organic matter and heavy metals (lead, copper, arsenic, etc.) can considerably affect  
379 the chemical properties and durability of concrete. Depending on the concentration of  
380 pollutants, it is advisable to use raw sediment classified as inert or non-hazardous  
381 material following the European directive 12/12/14/EC.
- 382 - Quantify the fine fraction of the RS. A percentage between 25 and 40% of fine  
383 particles below 125 µm is preferable. The results of the rheological properties have

- 384 shown that the presence of fine sediment particles leads to an increase in viscosity and  
385 a decrease in workability of the concrete. The rheological behavior of SCC depends  
386 strongly on the values of the shear stress. For an identical rheometer setting according  
387 to our study, it is recommended to have the following SCC paste shear stress values:
- 388     ▪ Between 20 and 25 Pa at 15 minutes after mixing for a W/B ratio = 0.46
  - 389     ▪ Between 15 and 20 Pa at 15 minutes after mixing for a W/B ratio = 0.48
- 390 - To determine the physical, chemical and mineralogical properties of the fine fraction  
391 of sediments. Knowledge of the water demand of the fine fraction as well as the type  
392 of clay present in the RS fines, allows the optimization of the formulation parameters,  
393 in particular the W/B ratio.
- 394 - Use less than 20% of raw sediment in the formulation of self-compacting concrete.  
395 This avoids the negative effects of sediment on the mechanical properties of the concrete and  
396 also allows optimization of the dosage of additives.
- 397 - Do not use viscosity enhancers for the formulation of self-compacting concrete based  
398 on RS from active lagoons. The hydrophobic nature of the clay in the sediment increases the  
399 stability of the concrete and improves its ability to resist the shear stresses induced by its  
400 weight.

## 401 **5 Conclusion**

402 To meet the ecological and raw material depletion objectives, we proposed and experimented  
403 with two formulations of SCC. These formulations include about 300 kg /m<sup>3</sup> of raw sediment.  
404 The purpose of this article is first to study the experimental feasibility of SCC without mineral  
405 addition but incorporating a high amount of raw sediment, then to analyze the impact of  
406 sediments on the rheological properties of SCC pastes. The relevant conclusions that emerge  
407 were:

- 408 - Non-hazardous sediment with an initial water content of 15 to 20% can be used at a  
409 high level to formulate SCC. The presence of the sediment ensures the good stability  
410 of the SCC. There is no segregation or bleeding in the fresh state. The 28-day  
411 compressive strengths confirm the use of RS-based concrete for nonstructural works.  
412 At the economic and ecological level, this result is particularly important because they  
413 are used in large quantities and require no physical and thermal treatment.

- 414 - The presence of RS increases the yield stress of SCC, there is a decrease in the  
415 mobility of SCC in an unconfined environment. RS fines do not have the same  
416 rheological behavior as other limestone mineral additions. The F1 fraction of the RS  
417 influences the water demand and superplasticizer of SCC. OM in SCC from sediment  
418 is also a major factor influencing the rheology of concrete.
- 419 - The dried state of the RS is not indicated for the formulation of SCC because after  
420 mixing, agglomerates can be observed which reduce the rheological and mechanical  
421 properties.

422 The densified mixture design algorithm (DMDA) based on the least void condition through  
423 the utilization of RS to fill the void between blended aggregates and cement paste to fill the  
424 rest of the void was used. To evaluate the influence of RS of the mix, a rheological study of  
425 comparison of yield stress accomplished made it possible to detect influential the parameters  
426 of the intrinsic properties of the raw sediment. The analysis of the results highlighted the real  
427 relevance of the OM and a fine fraction of RS, on the rheological properties of SCC  
428 formulated.

429 Extensive research is going on in our laboratories to increase the mechanical properties and  
430 durability of SCC based on raw sediment.

#### 431 **Ethical Approval**

432 'Not applicable'

#### 433 **Consent to Participate**

434 'Not applicable'

#### 435 **Consent to Publish**

436 'Not applicable'

#### 437 **Authors Contributions**

438 ' Nongwendé Philippe OUEDRAOGO: Conceptualisation, Data curation, Formal analysis,  
439 Methodology, Validation, Writing - original draught, Writing - review & editing. Frédéric  
440 Becquart: Validation, Resources, Supervision, Funding acquisition, Writing - review &  
441 editing. Mahfoud Benzzerzour: Validation, Resources, Supervision, Funding acquisition. Nor-  
442 Edine. ABRIAK: Validation, Resources, Project administration's

#### 443 **Funding**

444 'Not applicable'



445 **Competing Interests**

446 'The authors declare that they have no known competing financial interests or personal  
447 relationships that could have appeared to influence the work reported in this paper.'

448 **Availability of data and materials**

449 'The datasets used and/or analysed during the current study are available from the  
450 corresponding author on reasonable request'.

451 **Acknowledgements**

452 Authors would like to acknowledge the IMT Lille Douai for research funds.

453 **References**

- 454 [1] H. Okamura, K. Ozawa, and M. Ouchi, "Self-compacting concrete," *Struct. Concr.*,  
455 vol. 1, no. 1, pp. 3–17, 2000.
- 456 [2] C. Shi, Z. Wu, K. Lv, and L. Wu, "A review on mixture design methods for self-  
457 compacting concrete," *Constr. Build. Mater.*, vol. 84, pp. 387–398, 2015.
- 458 [3] J. M. D'ALOIA SCHWARTZENTRUBER, Laetitia and Torrenti, *Le grand livre des*  
459 *bétons*. ÉDITIONS LE MONITEUR, 2014.
- 460 [4] C. L. G. P. Raujouan, "Enquête Dragage 2010 - Synthèse des données, Centre d'Études  
461 Techniques Maritimes Et Fluviales (CETMEF)," 2013.
- 462 [5] V. Dubois, N. E. Abriak, R. Zentar, and G. Ballivy, "The use of marine sediments as a  
463 pavement base material," *Waste Manag.*, vol. 29, no. 2, pp. 774–82, Feb. 2009.
- 464 [6] H. Van Damme, "Cement and Concrete Research Concrete material science : Past ,  
465 present , and future innovations ☆," *Cem. Concr. Res.*, vol. 112, no. May, pp. 5–24,  
466 2018.
- 467 [7] P. de C. Predis Calais and G. de travail N°5, "Améliorer la valorisation des déchets  
468 industriels en BTP," 2006.
- 469 [8] I. Ennahal, W. Maherzi, Y. Mamindy, P. Mahfoud, B. Nor, and E. Abriak, "Eco-  
470 friendly polymers mortar for floor covering based on dredged sediments of the north of  
471 France," *J. Mater. Cycles Waste Manag.*, vol. 0, no. 0, p. 0, 2019.
- 472 [9] R. Achour, "Valorisation et caractérisation de la durabilité d 'un matériau routier et d  
473 'un béton à base de sédiments de dragage," *Thèse Dr. Univ. Lille*, p. 199, 2013.
- 474 [10] F. K. Aoual, D. Kerdal, M. Ameer, B. Mekerta, and A. Semcha, "Durability of mortars  
475 made with dredged sediments," vol. 118, pp. 240–250, 2015.
- 476 [11] E. Canada, A. Gosselin, D. Blackburn, and M. Bergeron, "*Protocole d 'évaluation de*  
477 *la traitabilité des sédiments , des sols et des boues à l'aide des technologies*  
478 *minéralogiques*". 1999.
- 479 [12] A. P. N. B. P, "Groupe de travail 'Recommandations pour l'emploi des Bétons Auto-  
480 Plaçants,'" 2008.
- 481 [13] D. E. S. Ponts, E. T. Chaussees, and J. Chappuis, "These T. Sedran," 1999.

- 482 [14] K. Ouhba, L. Benamara, A. H. Hamoui, A. Hamwi, and M. D. Loye, "Conception of a  
483 synthesis pozzolan from sediment dams calcined ( Case : Gargar dams )," vol. 3, 2014.
- 484 [15] M. Benzerzour, M. Amar, and N. Abriak, "New experimental approach of the reuse of  
485 dredged sediments in a cement matrix by physical and heat treatment," *Constr. Build.  
486 Mater.*, vol. 140, pp. 432–444, 2017.
- 487 [16] T. A. Dang, S. Kamali-Bernard, and W. A. Prince, "Design of new blended cement  
488 based on marine dredged sediment," *Constr. Build. Mater.*, vol. 41, pp. 602–611, Apr.  
489 2013.
- 490 [17] Z. Zhao, M. Benzerzour, N. Abriak, D. Damidot, L. Courard, and D. Wang, "Use of  
491 uncontaminated marine sediments in mortar and concrete by partial substitution of  
492 cement," *Cem. Concr. Compos.*, vol. 93, no. July, pp. 155–162, 2018.
- 493 [18] T. A. Dang, S. Kamali-Bernard, and W. A. Prince, "Design of new blended cement  
494 based on marine dredged sediment," *Constr. Build. Mater.*, vol. 41, pp. 602–611, Apr.  
495 2013.
- 496 [19] M. Amar, M. Benzerzour, N. Abriak, and Y. Mamindy-pajany, "Study of the  
497 pozzolanic activity of a dredged sediment from Dunkirk harbour," *Powder Technol.*,  
498 vol. 320, pp. 748–764, 2017.
- 499 [20] M. Amar, "Towards the establishment of formulation laws for sediment-based  
500 mortars," *J. Build. Eng.*, vol. 16, no. August 2017, pp. 106–117, 2018.
- 501 [21] E. Rozière, M. Samara, A. Loukili, and D. Damidot, "Valorisation of sediments in self-  
502 consolidating concrete: Mix-design and microstructure," *Constr. Build. Mater.*, vol. 81,  
503 pp. 1–10, Apr. 2015.
- 504 [22] Z. Lafhaj *et al.*, "The use of the Novosol process for the treatment of polluted marine  
505 sediment," vol. 148, pp. 606–612, 2007.
- 506 [23] Z. Lafhaj, M. Samara, F. Agostini, L. Boucard, F. Skoczylas, and G. Depelsenaire,  
507 "Polluted river sediments from the North region of France: Treatment with Novosol®  
508 process and valorization in clay bricks," *Constr. Build. Mater.*, vol. 22, no. 5, pp. 755–  
509 762, May 2008.
- 510 [24] Franck Agostini, Thèse de doctorat Ecole Centrale De Lille, "Inertage et valorisation  
511 des sédiments de dragage marins," 2007.
- 512 [25] Z. Lafhaj, Z. Duan, I. Bel Hadj Ali, and G. Depelsenaire, "Valorization of treated river  
513 sediments in self compacting materials," *Waste and Biomass Valorization*, vol. 3, no. 2,  
514 pp. 239–247, 2012.
- 515 [26] R. Snellings *et al.*, "Properties and pozzolanic reactivity of flash calcined dredging  
516 sediments," *Appl. Clay Sci.*, vol. 129, pp. 35–39, Aug. 2016.
- 517 [27] J. Ramaroson, "Calcination des sédiments de dragage contaminés. Etudes des  
518 propriétés physico-chimiques," p. 181, 2008.
- 519 [28] J. Couvidat, M. Benzaazoua, V. Chatain, and H. Bouzahzah, "Environmental  
520 evaluation of dredged sediment submitted to a solidification stabilization process using  
521 hydraulic binders," *Environ. Sci. Pollut. Res.*, vol. 23, no. 17, pp. 17142–17157, 2016.

- 522 [29] J. Couvidat, M. Benzaazoua, V. Chatain, A. Bouamrane, and H. Bouzahzah,  
523 “Feasibility of the reuse of total and processed contaminated marine sediments as fine  
524 aggregates in cemented mortars,” *Constr. Build. Mater.*, vol. 112, pp. 892–902, Jun.  
525 2016.
- 526 [30] P. Ozer-Erdogan, H. M. Basar, I. Erden, and L. Tolun, “Beneficial use of marine  
527 dredged materials as a fine aggregate in ready-mixed concrete: Turkey example,”  
528 *Constr. Build. Mater.*, vol. 124, pp. 690–704, 2016.
- 529 [31] L. Ben Allal, M. Ammari, I. Frar, A. Azmani, P. Clastres, and S. Jullien, “Stabilization  
530 of contaminated canal sediments,” *Eur. J. Environ. Civ. Eng.*, vol. 15, no. 2, pp. 293–  
531 302, 2011.
- 532 [32] W. P. Limited, *Understanding the rheology of concrete*. .
- 533 [33] D. W. Pribyl, “Geoderma A critical review of the conventional SOC to SOM  
534 conversion factor,” *Geoderma*, vol. 156, no. 3–4, pp. 75–83, 2010.
- 535 [34] A. Perrot, T. Lecompte, H. Kheli, C. Brumaud, J. Hot, and N. Roussel, “Cement and  
536 Concrete Research Yield stress and bleeding of fresh cement pastes,” vol. 42, pp. 937–  
537 944, 2012.
- 538 [35] P. Chang, C. Hwang, and Y. Peng, “Application of High-Performance Concrete to  
539 High-Rise Building in Taiwan,” vol. 4, no. 2, pp. 65–73, 2001.
- 540 [36] C. L. Hwang, M. F. Hung, and Y. Y. Chen, “Comparison of ACI Mixture Design  
541 Algorithm to HPC Desified Mixture Design Algorithm in the Anti-corrosion and  
542 Durability Design,” *J. Chinese Corros. Eng.*, vol. 16, no. 4, pp. 281–296, 2002.
- 543 [37] Y. Chen, B. Le, A. Tuan, and C. Hwang, “Effect of paste amount on the properties of  
544 self-consolidating concrete containing fly ash and slag,” *Constr. Build. Mater.*, vol. 47,  
545 pp. 340–346, 2013.
- 546 [38] F. De Larrard, F. Bosc, C. Catherine, and F. Deflorenne, “The AFREM method for the  
547 mix design of high performance concrete,” vol. 30, no. September, pp. 439–446, 1997.
- 548 [39] L. Ducloué *et al.*, “Yielding and flow of foamed metakaolin pastes To cite this version :  
549 HAL Id : hal-01205614 Yielding and flow of foamed metakaolin pastes,” 2015.
- 550 [40] N. Roussel, C. Stefani, and R. Leroy, “From mini-cone test to Abrams cone test :  
551 measurement of cement-based materials yield stress using slump tests,” vol. 35, pp.  
552 817–822, 2005.
- 553 [41] K. Hung, U. J. Alengaram, M. Zamin, S. Cheng, W. Inn, and C. Wah, “Recycling of  
554 seashell waste in concrete : A review,” *Constr. Build. Mater.*, vol. 162, pp. 751–764,  
555 2018.
- 556 [42] C. Martínez-garcía, B. González-fonteboa, F. Martínez-abella, and D. C.- López,  
557 “Virtual Special Issue Bio Based Building Materials Performance of mussel shell as  
558 aggregate in plain concrete,” vol. 139, pp. 570–583, 2017.

## List of figures

Fig 1 Granular separation process of the raw sediment into F1 and F2 fractions

Fig 2 Particle size distribution. (A1): cement, raw sediments, filler, sand. (A2): sand, coarse aggregate

Fig 3 Schematic representation of the discretisation model.

Fig. 4. Organisation charts of method applied to study SSC, grout and paste.

Fig. 5. Mixing protocol for SCC-equivalent paste

Fig. 6. The rheological measurements. (A1): Anton Paar Modular Compact Rheometer MCR 102. (A2): Examples of transient flow behaviours.

Fig. 7. Curves obtained in the different grouts. (A1): the saturation doses of superplasticizer. (A2): slump test measured with mini-cone for Sp were 0.72, 0.52% for F1G, F2G respectively

Fig. 8. Demonstration of the presence of sediment agglomerates during shear stress measurements of pastes

Fig. 9. Properties of self-consolidating concretes. (A1): slump tests using the Abrams cone. (A2): cylindrical to determine the compressive strength

Fig. 10. (A1): compressive strength development of concrete specimens. (A2): tensile strength development of concrete specimens.

Fig. 11. Shear stress vs. strain for a yield stress measurement at low shear rate in different pastes. W/B ratio from 0.46 (A1: WS, A2: WC, A3: WF); W/B = 0.48 (B1: WS, B2: WC, B3: WF).

Fig. 12. Shear stress vs. strain for a yield stress measurement at low shear rate in different pastes. W/B ratio from 0.46 (A4: WCS<sub>ed</sub>, A5: WCF, A6: WCS<sub>edSSp</sub>); W/B = 0.48 (B4: WCS<sub>ed</sub>, B5: WCF, B6: WCS<sub>edSSp</sub>)

Fig. 13. Development with time after mixing of the static yield stress, for pastes. W/B ratios from 0.46 for (C1), (C2) (C3) and W/B ratios from 0.48 for (D1) (D2) (D3).

Fig. 14. Development with time after 45 minutes mixing of plastic viscosities

Fig. 15. slump tests using the mini-cone. (A1): slump for F1P, (A2): slump for F2P

Fig. 16. SEM micrographs of raw sediment

Fig. 17. SEM micrographs of SCC paste

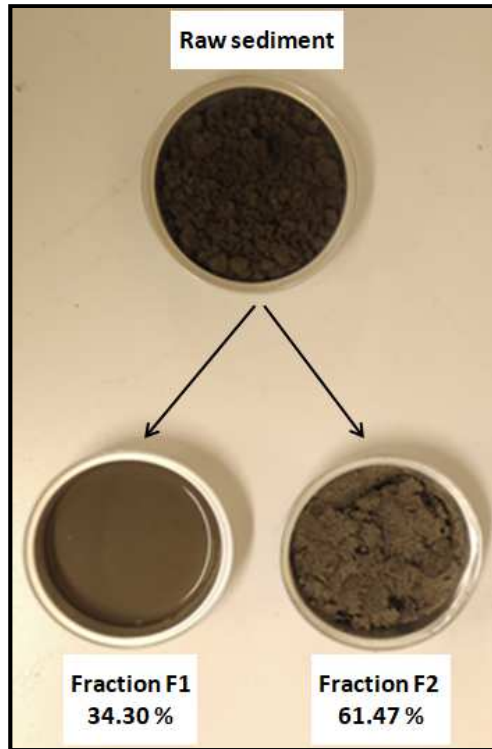


Fig. 5. Granular separation process of the raw sediment into F1 and F2 fractions

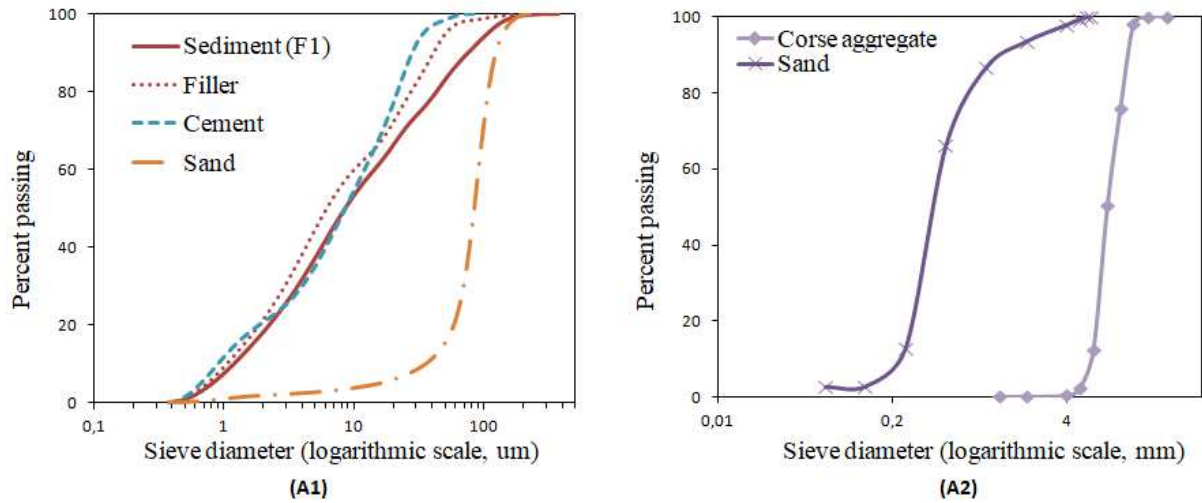


Fig. 6. Particle size distribution. (A1): cement, raw sediments, filler, sand. (A2): sand, coarse aggregate

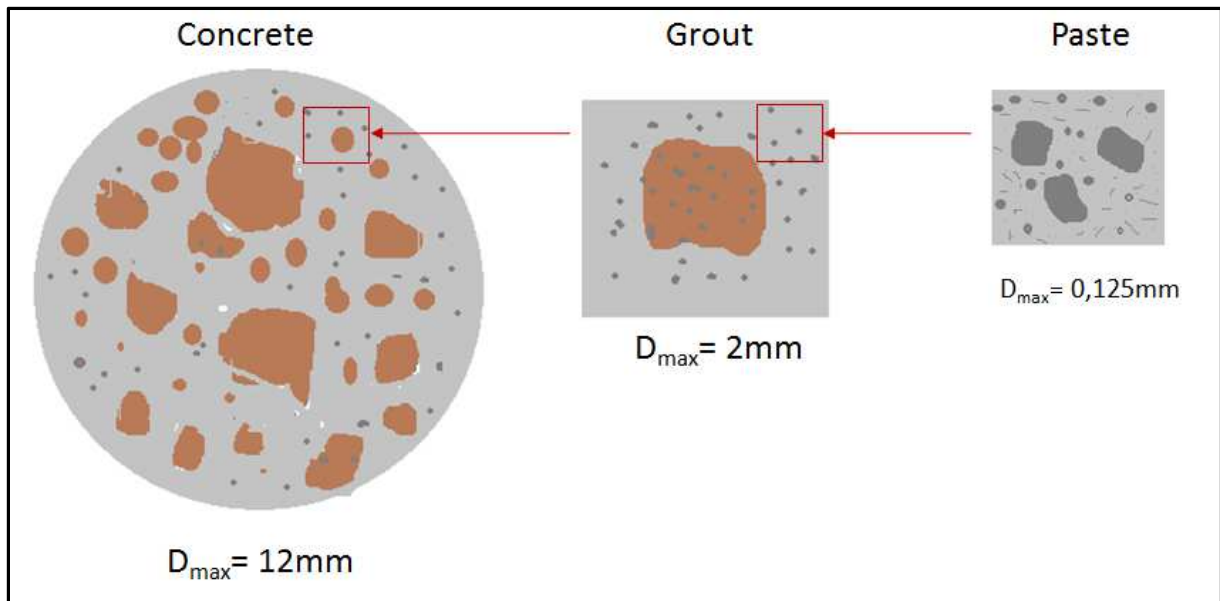


Fig. 7. Schematic Representation of the Discretisation Model

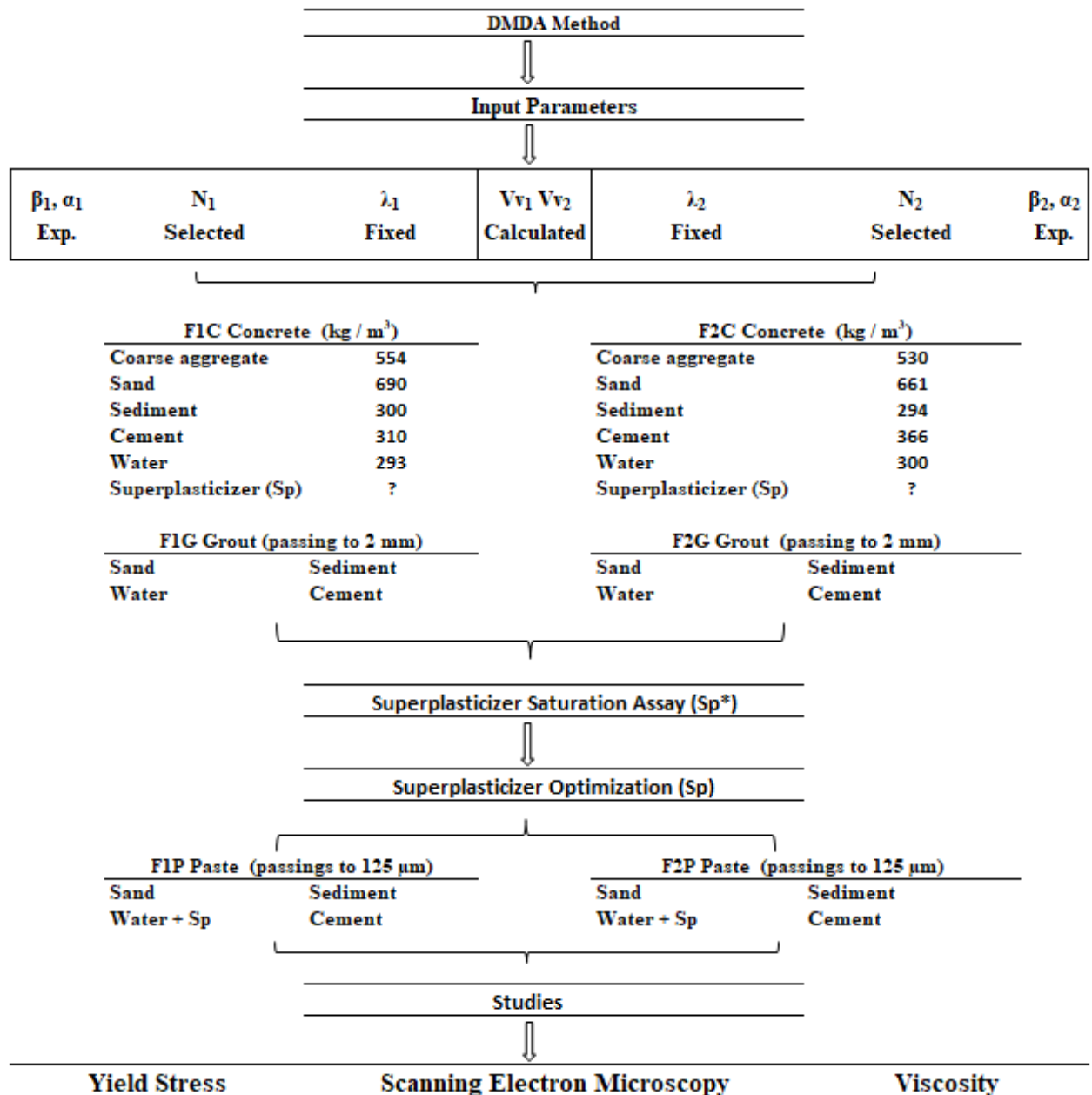


Fig. 8. Organisation chart of method applied to study SSC, grout and paste

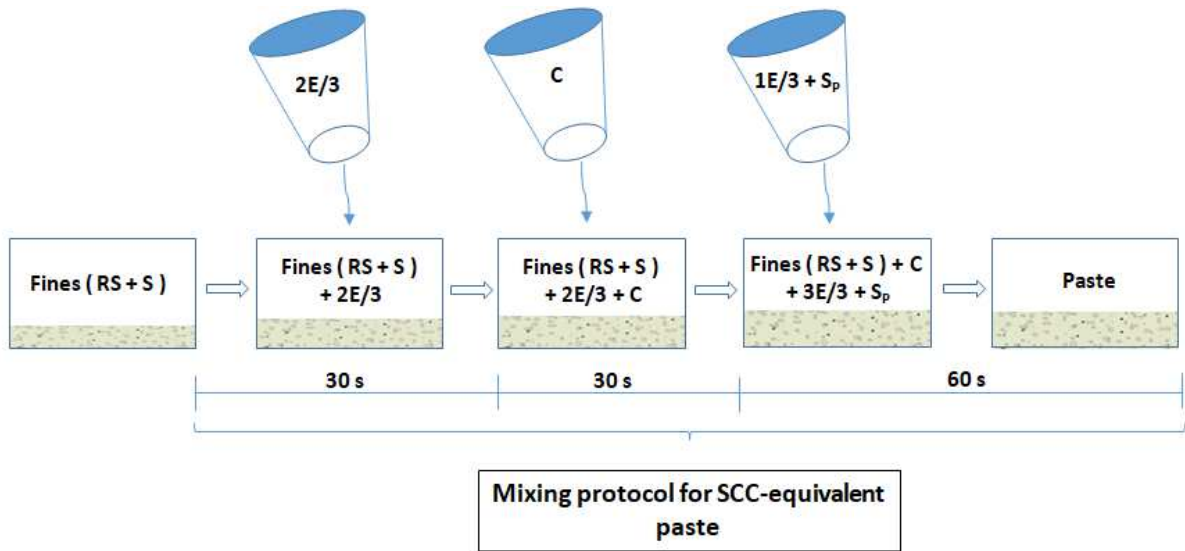


Fig. 5. Mixing protocol for SCC-equivalent paste

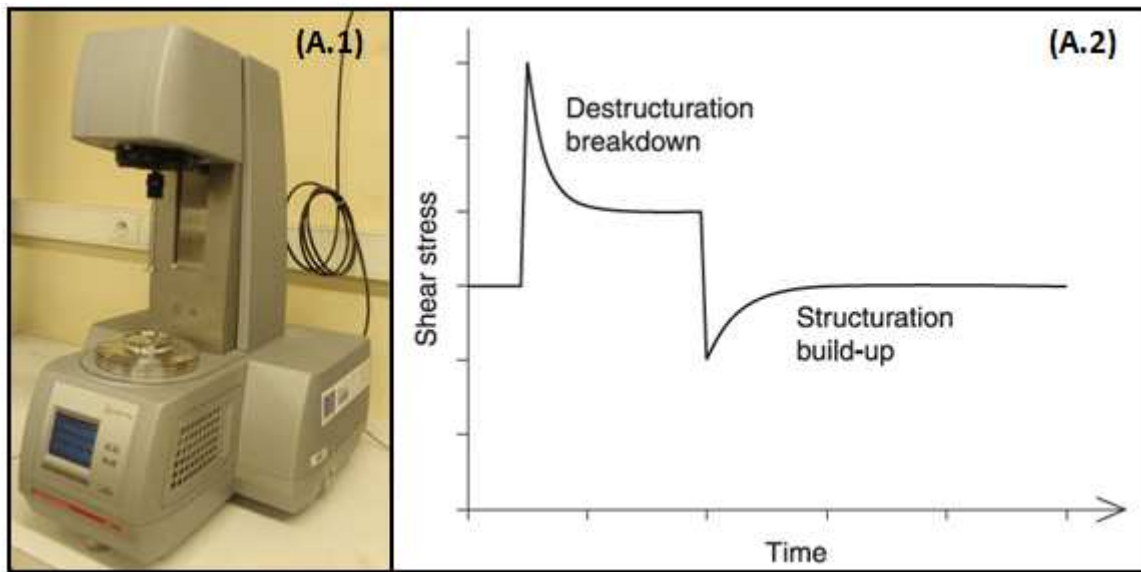


Fig. 6. The rheological measurements. (A1): Anton Paar Modular Compact Rheometer MCR 102. (A2): Examples of transient flow behaviours



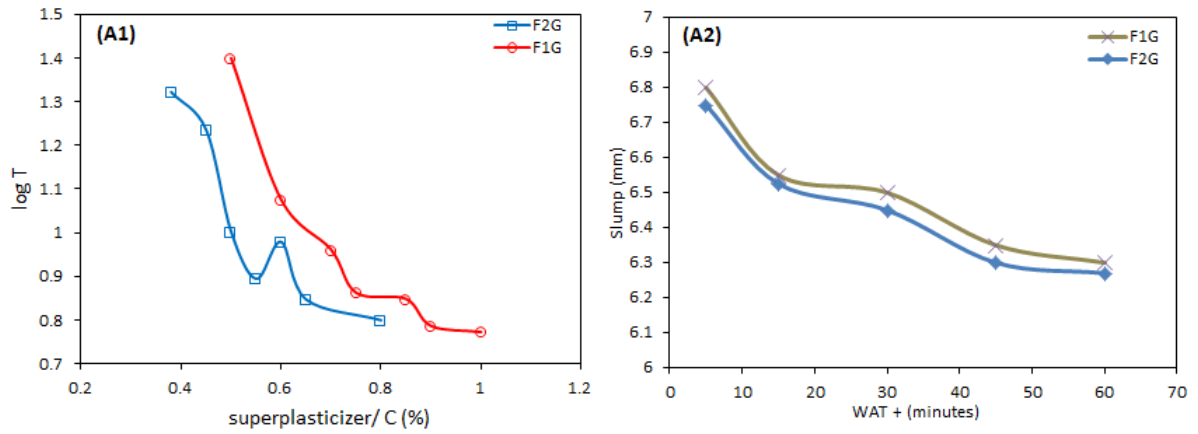


Fig. 7. Curves obtained in the different grouts. (A1): the saturation doses of superplasticizer. (A2): slump test measured with mini-cone for Sp was 0.72, 0.52% for F1G, F2G respectively

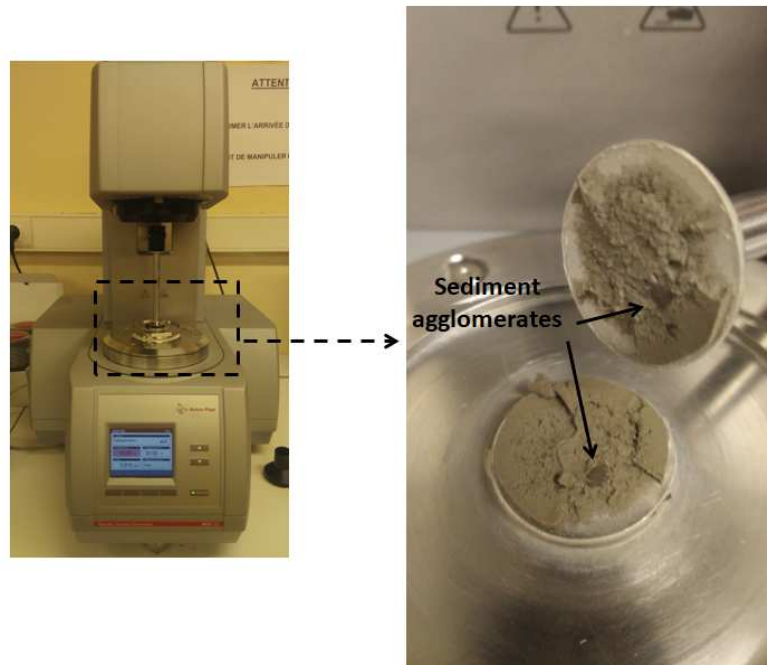


Fig. 8. Demonstration of the presence of sediment agglomerates during shear stress measurements of pastes

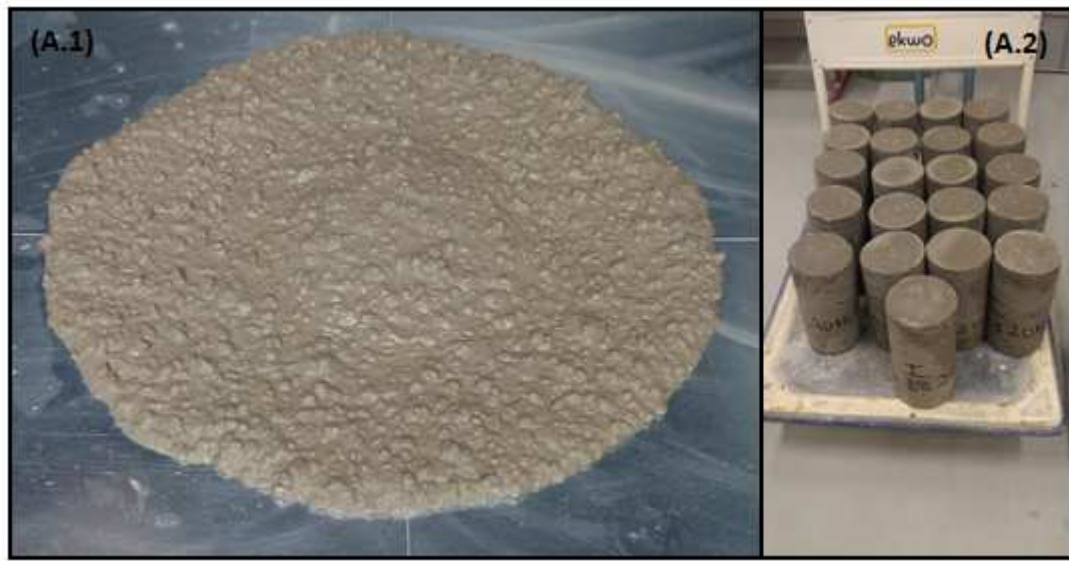


Fig. 9. Properties of self-consolidating concretes. (A1): slump tests using the Abrams cone. (A2): cylindrical to determine the compressive strength

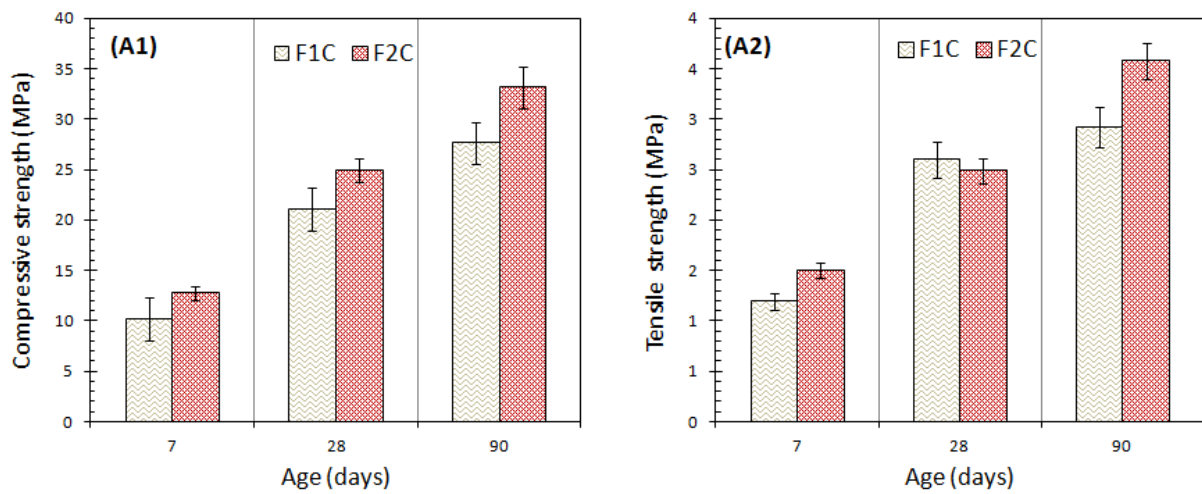


Fig. 10. (A1): compressive strength development of concrete specimens. (A2): tensile strength development of concrete specimens

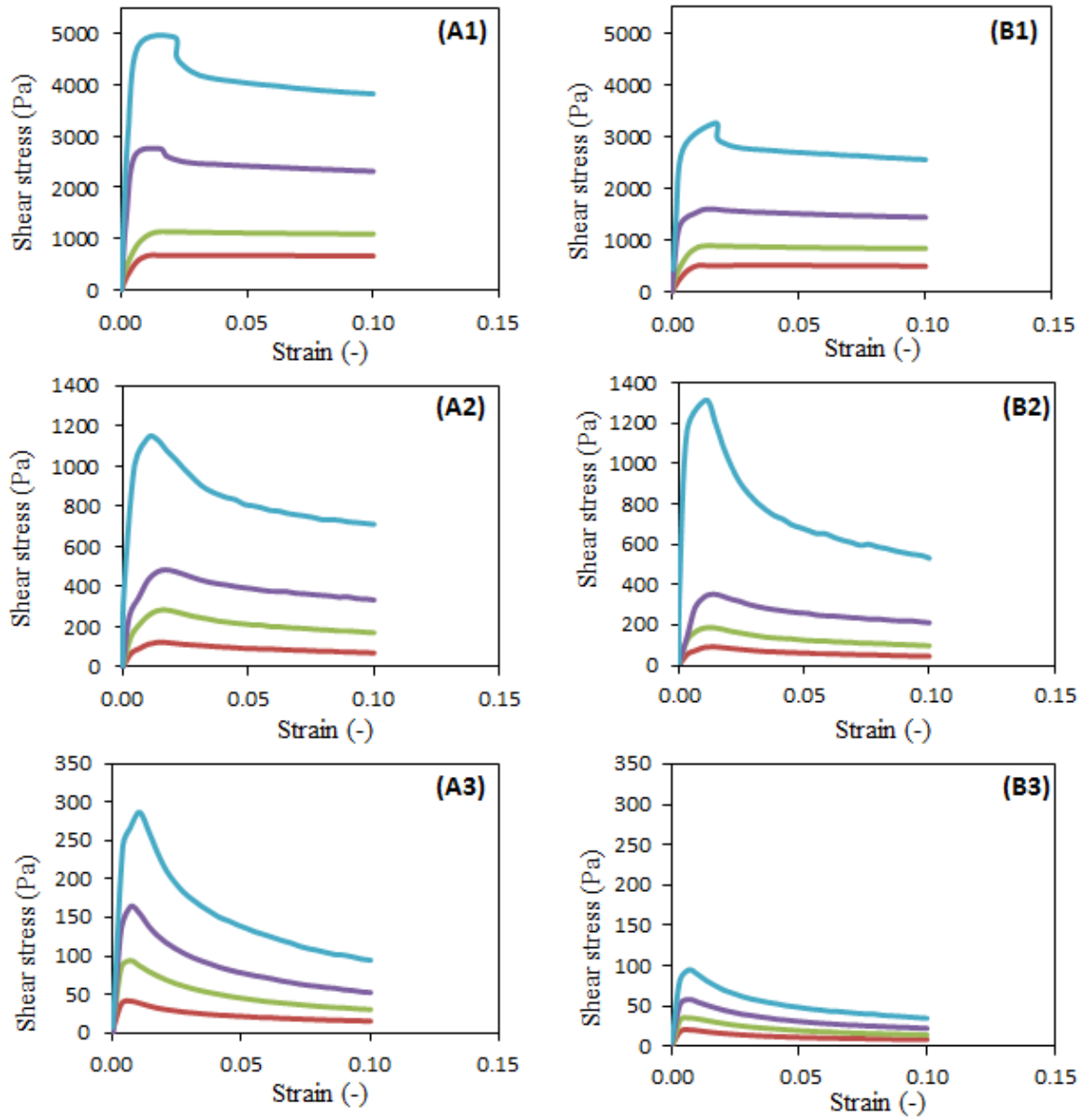


Fig. 11. Shear stress vs. strain for a yield stress measurement at low shear rate in different pastes. W/B ratio from 0.46 (A1: WS, A2: WC, A3: WF); W/B = 0.48 (B1: WS, B2: WC, B3: WF)

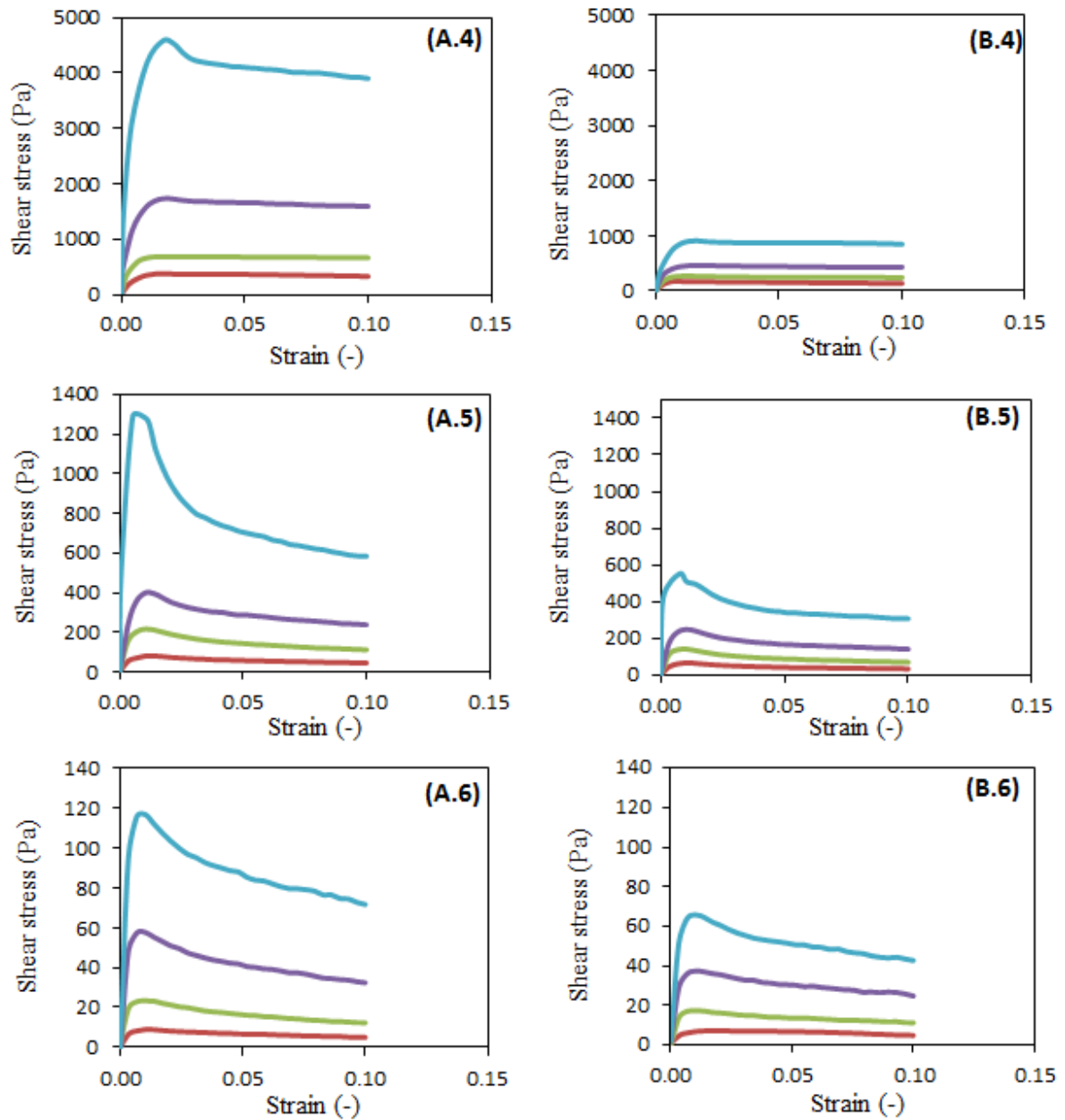


Fig. 12. Shear stress vs. strain for a yield stress measurement at low shear rate in different pastes. W/B ratio from 0.46 (A4: WCSed, A5: WCF, A6: WCSedSSp); W/B = 0.48 (B4: WCSed, B5: WCF, B6: WCSedSSp)

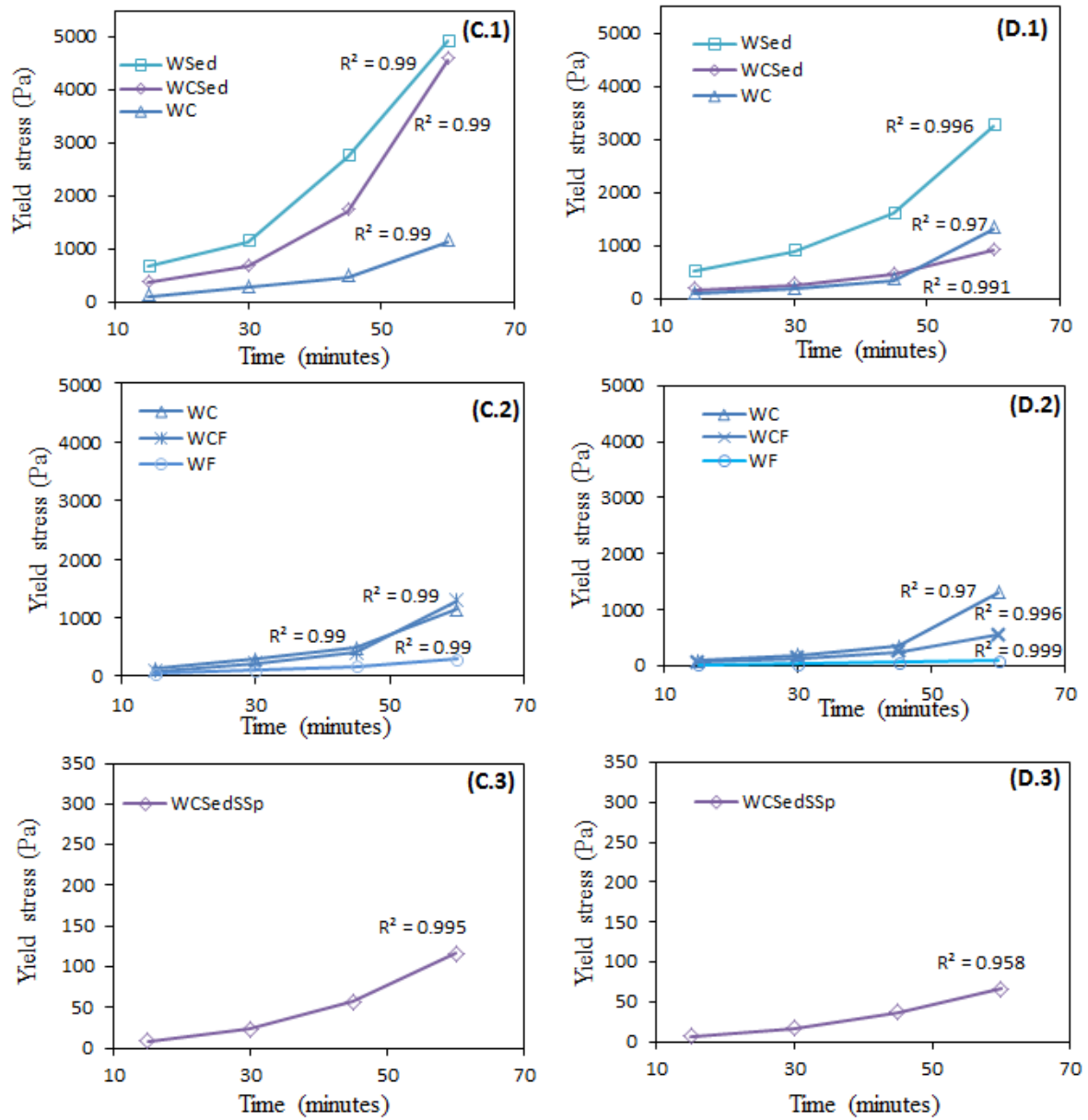


Fig. 13. Development with time after mixing of the static yield stress, for pastes. W/B ratios from 0.46 for (C1), (C2) (C3) and W/B ratios from 0.48 for (D1) (D2) (D3)

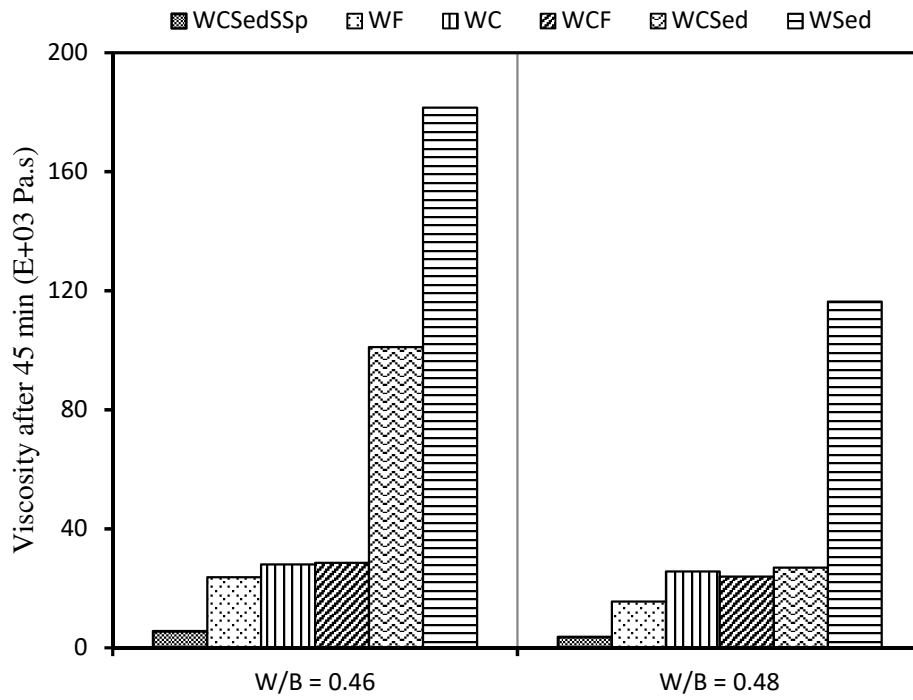


Fig. 14. Development with time after 45 minutes mixing of plastic viscosities

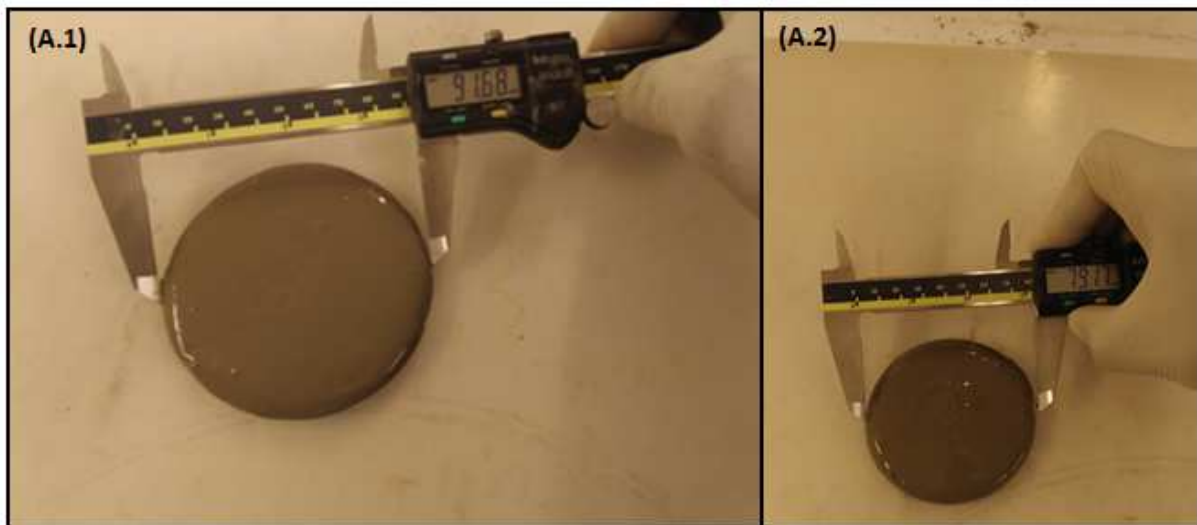


Fig. 15. slump tests using the mini-cone. (A1): slump for F1P, (A2): slump for F2P

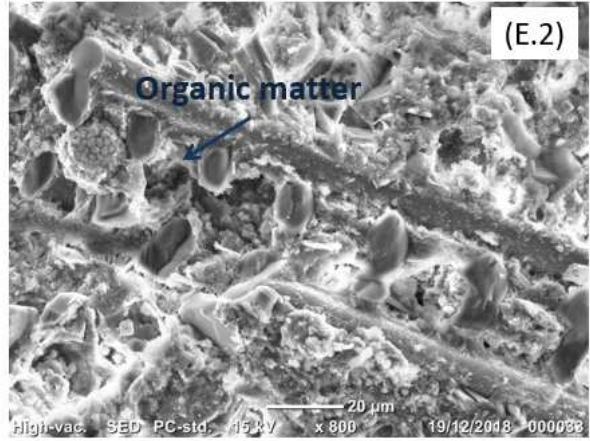
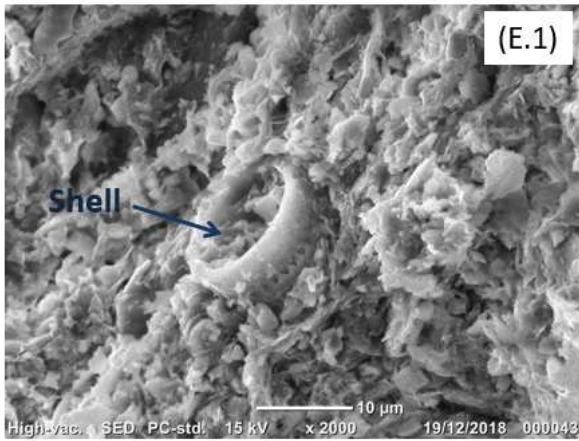


Fig. 16. SEM micrographs of raw sediment

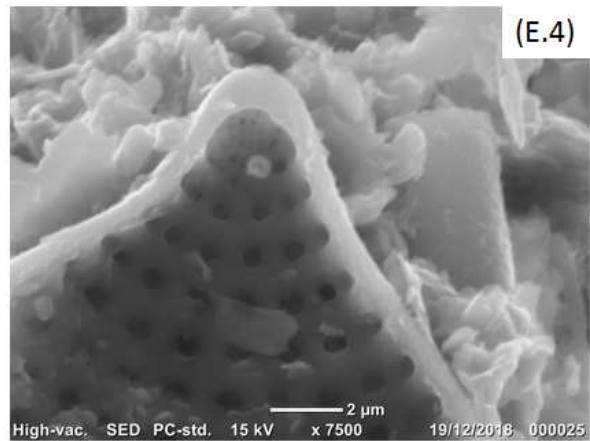
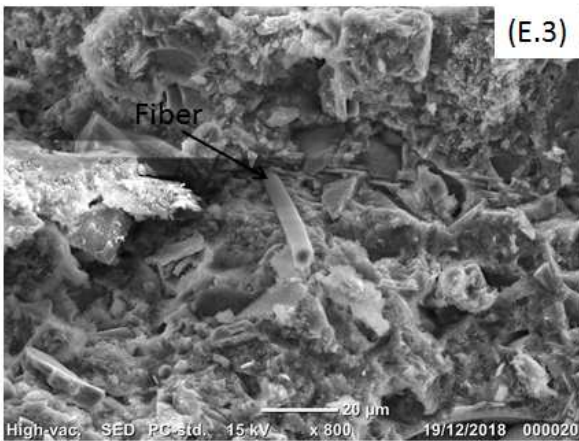
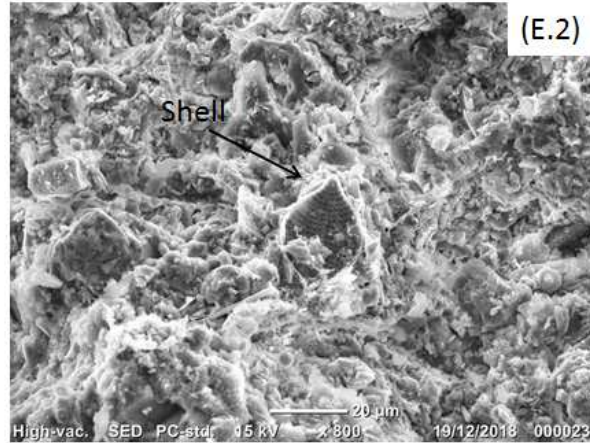
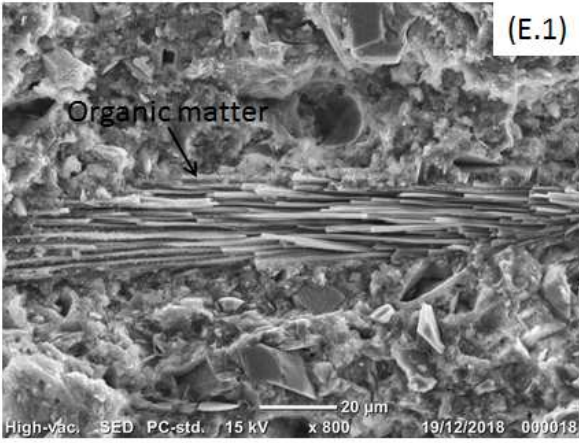


Fig. 17. SEM micrographs of SCC paste

## **List of Tables**

Table 1. Physical properties of coarse aggregates and sand

Table 2. Oxide composition of cement and raw sediments using XRF (%)

Table 3. Leaching test results and limiting values of classification of wastes from 28 October 2010/CE

Table 4. Mix proportioning of concrete, grout and paste.

Table 5. Mix percentage of coarse aggregate, sand, sediment, and cement in the granular matrix

Table 6. Paste nomenclature for  $W/B = 0.46$  and  $W/B = 0.48$



Table 7. Physical properties of coarse aggregates and sand

Physical properties	Natural aggregates	
	Corse (4/11.2 mm)	Sand (0/4 mm)
Specific gravity	2.45	2.64
Bulk density (kg/m <sup>3</sup> )	1456	1718
Micro-Deval test (%)	11	/
Los Angeles abrasion test(%)	21	/
Fineness modulus	/	2.72
Absorption capacity (%)	0.43	1.1

Table 8. Oxide composition of cement and raw sediments using XRF (%)

Oxides composition	Materials	
	Raw sediments	CEM III 42.5 N
SiO <sub>2</sub>	56.39	26.1
Al <sub>2</sub> O <sub>3</sub>	4.70	7.8
MgO	0.91	3.4
Fe <sub>2</sub> O <sub>3</sub>	1.95	2.2
CaO	12.75	55
Na <sub>2</sub> O	1.22	0.32
K <sub>2</sub> O	1.16	-
P <sub>2</sub> O <sub>5</sub>	0.20	-
SO <sub>3</sub>	0.90	2.03
TiO <sub>2</sub>	0.19	-
MnO	Trace	-
ZnO	Trace	-

Table 9. Leaching test results and limiting values of classification of wastes from 28 October 2010/CE

Heavy metals mg/kg dry mass	Raw sediment	Inert	Non-Dangerous	Dangerous
Barium	27.47	20	100	300
Chromium	0.17	0.5	10	70
Copper	4.69	2	50	100
Nickel	0.23	0.4	10	40
Lead	0.13	0.5	10	50
Zinc	0.55	4	50	200
Cadmium	0.035	0.04	1	5
Molybdenum	2.71	0.5	10	30
Arsenic	0.51	0.5	2	25

Mercury	<0.0010	0.01	0.2	2
---------	---------	------	-----	---

Table 10. Mix proportioning of concrete, grout and paste

materials of SCC mixtures 1 m <sup>3</sup>	Mixture label					
	F1C	F1G	F1P	F2C	F2G	F2P
Cement CEM III / A (kg)	310	396	838	366	460	933
Coarse aggregate (kg)	554	-	-	530	-	-
Sand (kg)	690	824	43	661	778	48
Sediment (kg)	300	383	318	294	371	289
Water (kg)	293	374	556	300	378	562
Efficient water (kg)	236	301	449	246	309	456
Superplasticizer (kg)	11	14	30	10	12	24
W/C	0.94	0.94	0.66	0.82	0.82	0.60
W <sub>eff</sub> /C	0.76	0.76	0.53	0.67	0.67	0.48
W/B = W/(C + S <sub>ed</sub> )	0.48	0.48	0.48	0.46	0.46	0.46
W <sub>eff</sub> /(C + S <sub>ed</sub> )	0.39	0.39	0.39	0.37	0.37	0.37
S <sub>p</sub> /C (%) dry extract of cement mass	0.72	0.72	0.72	0.52	0.52	0.52
N	1.164	1.164	1.164	1.190	1.190	1.189
Total fine content < 125 μm (%)	24	35	100	27	39	100
Sediment fines content < 125 μm (%)	6	9	100	6	9	100

Table 11. Mix percentage of coarse aggregates, sand, sediment, and cement in the dry granular matrix

Percentages of the various components determined by DMDA.	Mixture label					
	F1C	F1G	F1P	F2C	F2G	F2P
Cement	17	25	69.9	20	29	73.5
Sediment	16	24	26.6	16	23	22.8
Coarse aggregate	30	0	0.0	29	0	0.0
Sand	37	51	3.6	36	48	3.7

Table 12. Paste nomenclature for W/B = 0.46 and W/B = 0.48

Nomenclature	Paste Symbols
W/C	Water/Cement WC
W/S <sub>ed</sub>	Water/Sediment W <sub>Sed</sub>
W/F	Water/ Filler WF
W/B = W/(C+S <sub>ed</sub> )	Water/(Cement+Sediment) WCS <sub>ed</sub>

---

$W/C+F$	Water/(Cement+Filler)	WCF
$W/C+S_{ed}+S$	Water/(Cement+Sediment+Sand)	$WCS_{ed}S$
$W/C+S_{ed}+S+S_p$	Water/(Cement+Sediment+Sand+Superplasticizer)	$WCS_{ed}SS_p$

---

# Graphical Abstract

